V31B-4751

Advanced Seismic Studies of the Endeavour Segment of the Juan de Fuca Ridge: Understanding the Interplay among Magmatic, Hydrothermal, and Tectonic Processes at Mid-Ocean Ridges

Gillean M. Arnoux[1*], Brandon P. Vanderbeek[1], Joanna V. Morgan[2], Emilie E. E. Hooft[1], Douglas R. Toomey[1], William S. D. Wilcock[3], and Michael Warner[2]

[1]University of Oregon, Eugene, OR, [2]Imperial College London, London, SW7, United Kingdom, [3]University of Washington Seattle Campus, Seattle, WA, United States

*arnoux@uoregon.edu

I. Introduction

3D full-waveform inversion (FWI) is a state-of-the art seismic method developed for use in the oil industry to obtain high-resolution models of the subsurface velocity structure. The primary advantage of FWI is that it has the potential to resolve subsurface structures on the order of half the seismic wavelength—a significant improvement on conventional travel time tomography. Here, we apply anisotropic 3D FWI to data collected on the Endeavour segment of the Juan de Fuca Ridge.

II. ETOMO experiment

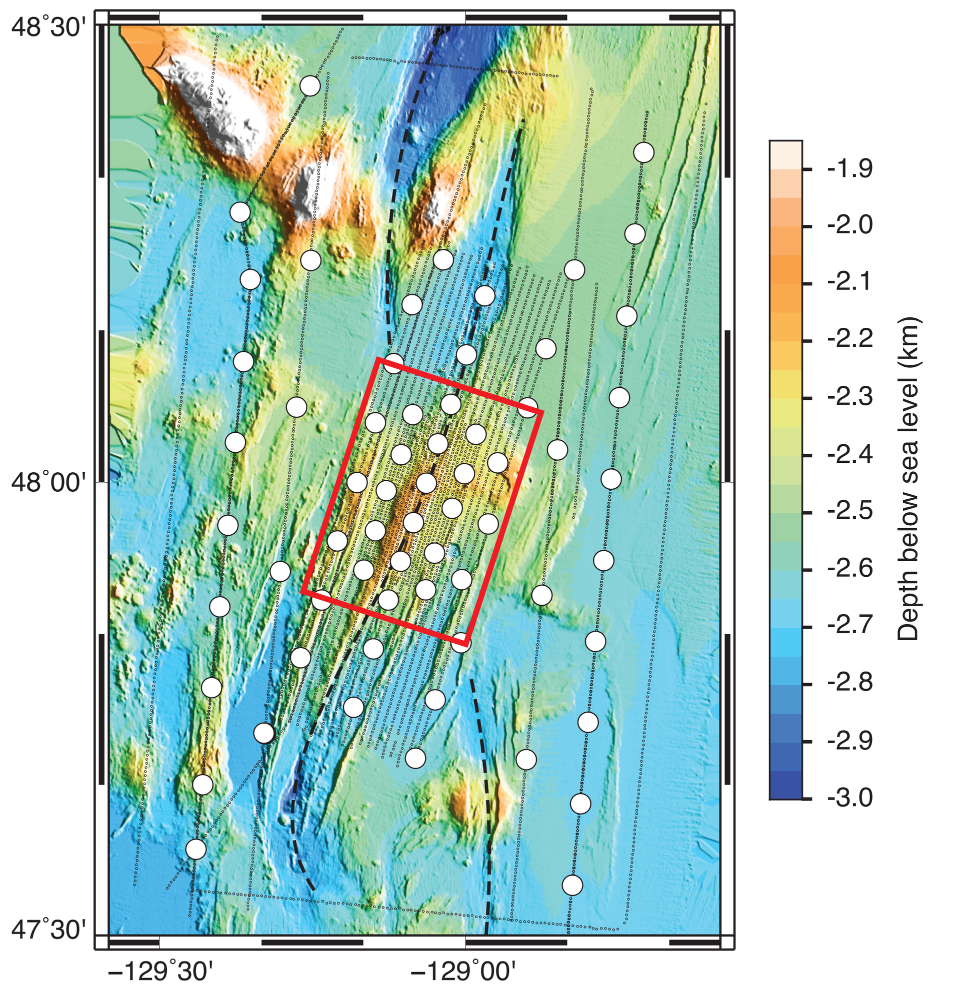

Figure 1: Map of the Endeavour segment of the Juan de Fuca Ridge from the Endeavour seismic tomography (ETOMO) experiment. Seismic data were collected using four-component ocean bottom seismometers (OBSs; white circles) and the 6600” airgun array of the R/V Marcus G. Langseth. Black circles show shot locations and thick dashed line shows the plate boundary. Data from the crustal grid (red box) were used for FWI.

III. Travel time tomography

- Weekly et al. (2014)[5] used travel time tomography to derive the isotropic and anisotropic P-wave velocity structure of the upper oceanic crust on the Endeavour segment. We use this starting model for anisotropic 3D FWI.

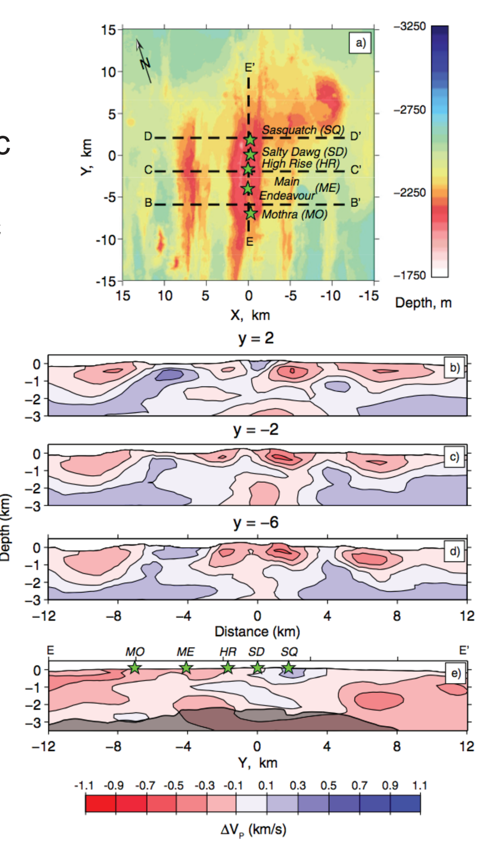

Figure 2: Vertical sections showing velocity anomalies for the central portion of the Endeavour Ridge. (a) Bathymetric map showing the locations of the vertical sections (dashed lines) shown in b-e, and known hydrothermal vent fields (labeled green stars). (b–d) Vertical sections crossing the ridge-axis at (b) Y = -6 km near the Mothra vent field, (c) Y = -2 km near the High Rise vent field, and (d) Y = 2 km near the Sasquatch vent field. (e) Vertical section along the ridge-axis showing vent fields (green stars) and the position of the top of the axial magma chamber (AMC; black solid line) obtained by converting two-way travel times to the AMC (Van Ark et al., 2007) to depth assuming the horizontally averaged velocity model from the inversion. From Weekly et al. (2014)[5].

IV. Data and methods

i. Full-waveform inversion (FWI)

- FWI is a technique that seeks to find a high-resolution, high fidelity, subsurface velocity model capable of matching the seismic field data, wiggle-for-wiggle, trace-by-trace.
- Uses an acoustic approximation to the wave equation and includes the kinematic effects of P-wave anisotropy[4]; the velocity model is updated iteratively and the anisotropy model is kept constant.

ii. Data quality

- Data from the ETOMO crustal grid is used for FWI. Of the 21 OBSs that recorded 1673 air gun shots, 19 recorded data useable for FWI. The phase of these data are range- and frequency-dependent.

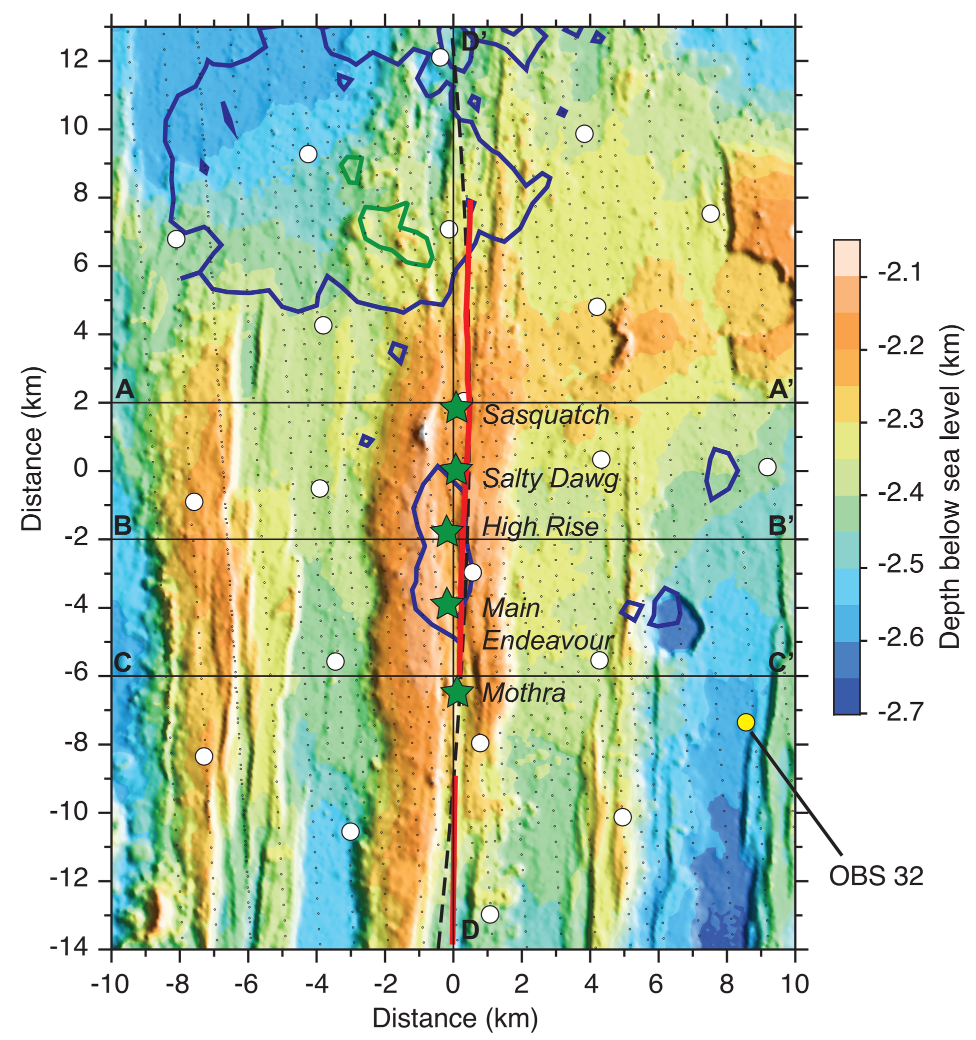

Figure 3: Map of the crustal grid (red box in Fig. 1). White circles are OBSs and black dots are shots used in FWI. Segment trace is shown by dashed black line. Green stars are hydrothermal vents and red segments are axial magma chamber locations[1,3]. Blue and green contours show areas with earthquake densities >5 and >24 events per km^2 [ref. 2], respectively. OBS 32 (labeled yellow circle) corresponds to the plots in Figs. 4 and 7. Black lines are vertical sections shown in Fig. 5.

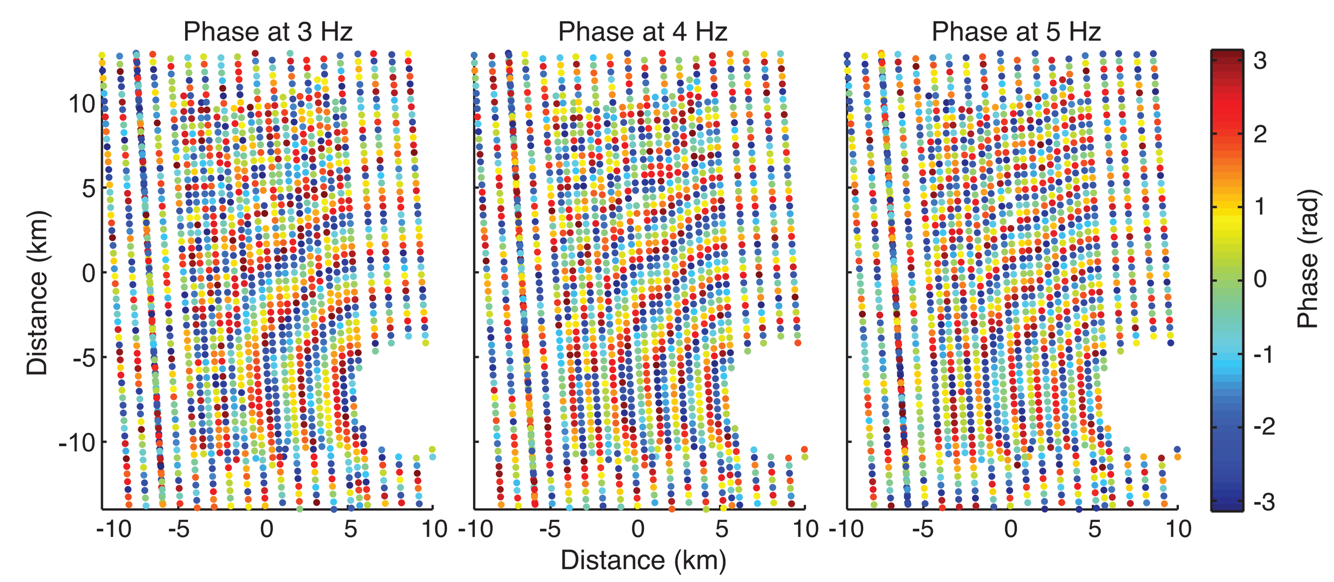

Figure 4: Phase variation with offset for a common receiver gather for the hydrophone on OBS 32 (yellow, annotated circle in Fig. 3) at 3, 4, and 5 Hz. Data are shown for all sources recorded within the model space (black dots in Fig. 3). The raw data have been Fourier transformed and the resultant phase for a single frequency is plotted in the physical location of the source recorded on the instrument. Spatial coherence, represented by concentric rings about the receiver, indicates source-generated signal usable for FWI, whereas graininess represents noisy data.

- A 700 ms window is applied to the data after the onset of the first arrival. Inversions use data within offsets of 2.9 and 15 km to limit the effect of noise.

Acknowledgements

The 3D FWI code used in this study was developed through industrial sponsorship managed by the Industry Technology Facilitator (ITF), UK. The experiment and analysis were supported by the NSF under grants numbered OCE-0454700 to the University of Washington and OCE-0454747 and OCE-0651123 to the University of Oregon.

References

1. Van Ark, E. M., R. S. Detrick, J. P. Canales, S. M. Carbotte, A. J. Harding, G. M. Kent, M. R. Nedimovic, W. S. D. Wilcock, J. B. Diebold, and J. M. Babcock (2007). Seismic structure of the Endeavour Segment, Juan de Fuca Ridge: Correlations with seismicity and hydrothermal activity. *Journal of Geophysical Research: Solid Earth (1978–2012), 112*(B2).
2. Hooft, E. E., Patel, H., Wilcock, W., Becker, K., Butterfield, D., Davis, E., ... & Stakes, D. (2010). A seismic swarm and regional hydrothermal and hydrologic perturbations: The northern Endeavour segment, February 2005. *Geochemistry, Geophysics, Geosystems, 11*(12).
3. Carbotte, S. M., J. P. Canales, M. R. Nedimovic, H. Carton, and J. C. Mutter (2012), Recent seismic studies at the East Pacific Rise 8°20– 10°10 N and Endeavour segment: Insights into mid-ocean ridge hydrothermal and magmatic processes, *Oceanography, 25*(1), 100–112.
4. Morgan, J., Warner, M., Bell, R., Ashley, J., Barnes, D., Little, R., Roele, K., and Jones, C. (2013). Next-generation seismic experiments: wide-angle, multi-azimuth, three-dimensional, full-waveform inversion. *Geophysical Journal International, 195*(3), 1657-1678.
5. Weekly, R. T., Wilcock, W. S., Toomey, D. R., Hooft, E. E., and Kim, E (2014). Upper crustal seismic structure of the Endeavour segment, Juan de Fuca Ridge from traveltime tomography: Implications for oceanic crustal accretion. *Geochemistry, Geophysics, Geosystems, 15*(4), 1296-1315.

V. Results

i. Velocity structure

- **FWI resolves larger-amplitude anomalies and more structure overall in comparison to conventional travel time tomography.**
- **Low-velocity anomalies beneath the ridge axis correlate with the location of a previously resolved, segmented axial magma chamber[1,3].**
- **All of the five known hydrothermal vent fields along the ridge are underlain by low-velocity anomalies, which likely represent thermal anomalies.**
- **The northernmost vent fields - High Rise, Salty Dawg, and Sasquatch - are also underlain by shallower high-velocity anomalies, potentially indicating reduced porosity caused by mineral precipitation.**
- **The northernmost low-velocity anomaly located <3 km beneath the ridge-axis (Figs. 5 and 6) may be the result of enhanced porosity caused by recent earthquake swarms in the region[2].**

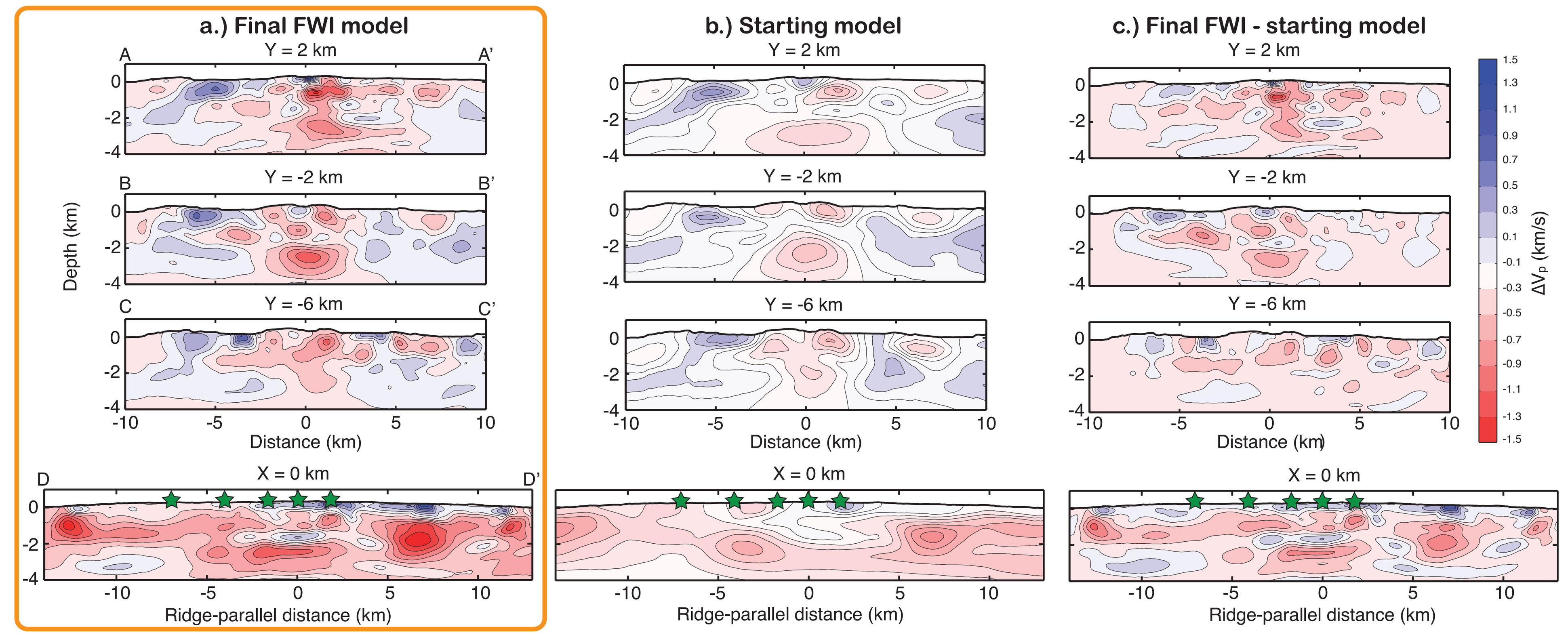

Figure 5: Vertical sections comparing velocity anomalies for the starting and final FWI models for the central portion of the Endeavour. Each plot has four vertical sections (three ridge-crossing and one ridge-parallel): Y = 2 km near the Sasquatch field, Y= -2 km near the High Rise field, Y= -6 near the Mothra field, and a ridge-parallel section showing vent fields (green stars). Locations of the vertical sections are shown in Figure 3. (a) Velocity anomalies for the final FWI model minus the 1D average from the starting model. (b)Velocity anomalies for the starting model minus the 1D average from the starting model. (c) Velocity anomalies corresponding to the final FWI model minus the starting model. The contour interval for velocity perturbations in (a) and (c) is 0.2 km/s, whereas the contour interval (b) is 0.1 km/s.

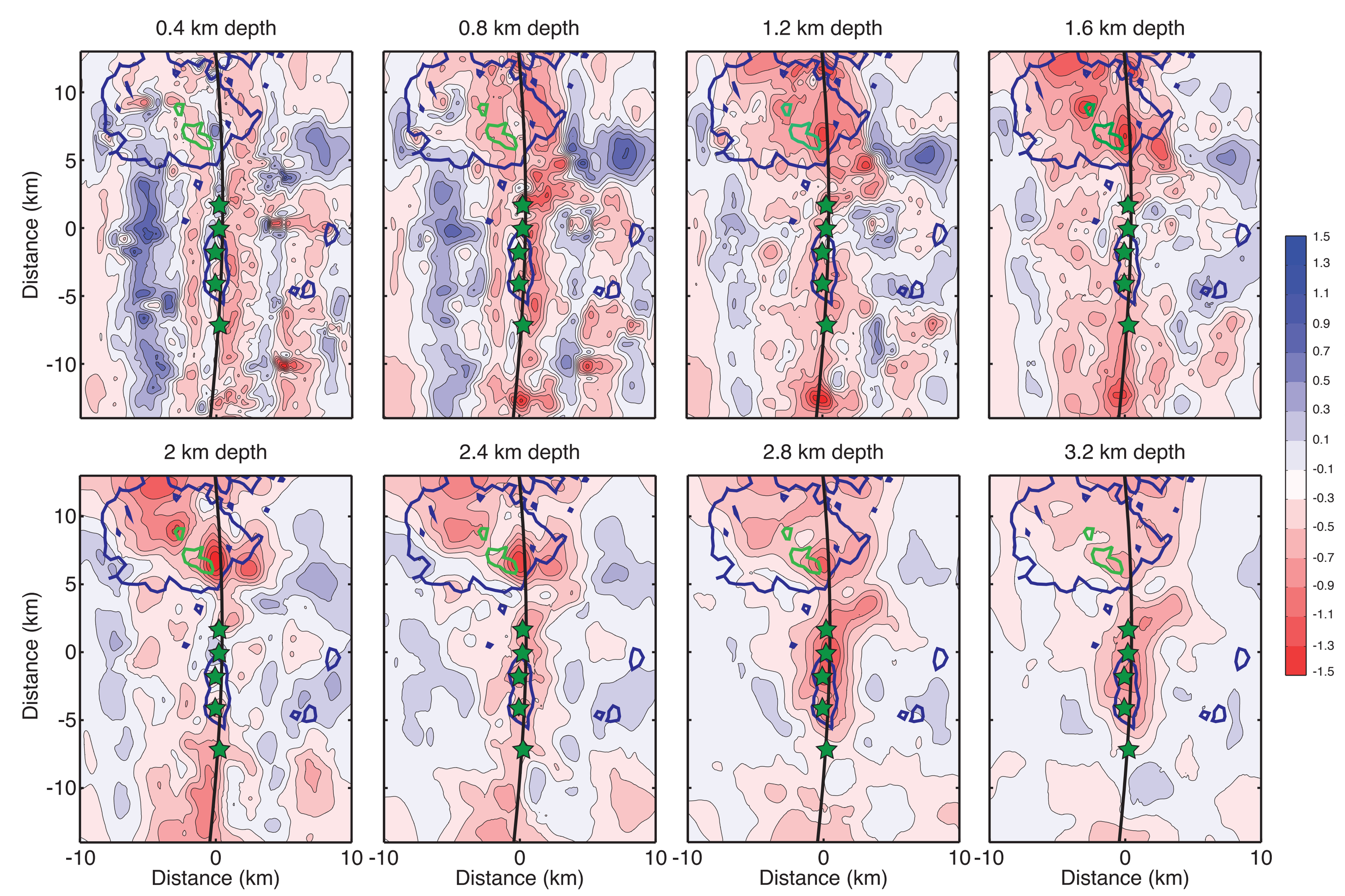

Figure 6: Map view sections of 3D segment-scale velocity anomalies relative to the horizontally averaged starting model. Horizontal slices of the inversion volume are presented at 0.4 km depth intervals.Velocity perturbations are contoured every 0.2 km/s.The Endeavour segment is shown by bold black lines,vent fields by green stars, and seismicity by contours (same as in Fig. 3).

ii. Model fit

- To judge the fit of the model, we view the phase match between the field data and synthetics generated using the final FWI model; amplitudes are normalized during the inversion, thus the amplitudes of the synthetics won't necessarily match those of the data.
- The final FWI model is capable of predicting the first 700 ms of data recorded from shots within 10 km of the receiver at both low (3 Hz) and high frequencies (up to 5.2 Hz). Data within 15 km offsets can also be matched at higher frequencies (up to 5.2 Hz).

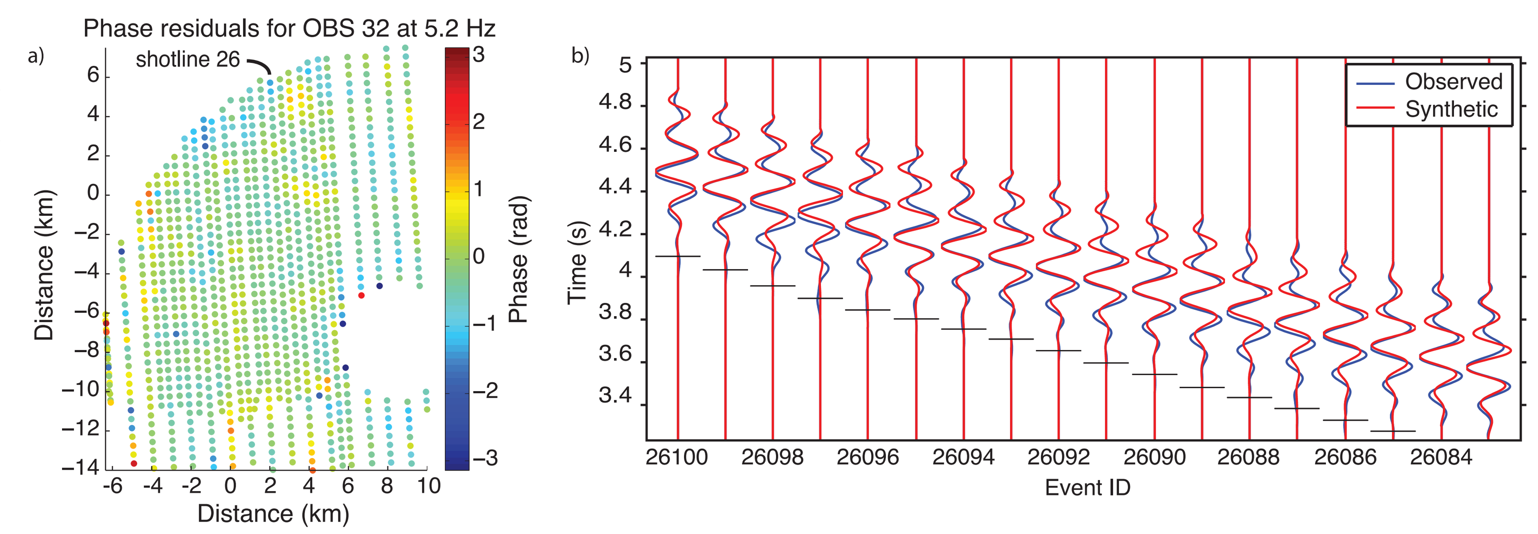

Figure 7: Phase residuals (synthetic minus observed) for shots recorded on OBS 32 and trace comparison for a sequence of events. (a) Phase residuals, in radians, for shots recorded on OBS 32 within 2.9 to 15 km offset from the receiver at 5.2 Hz. Residuals only take into account the first 700 ms of data after the onset of the first arrival. Events from shotline 26 (labeled) are shown in (b). (b) Comparison of observed (blue) and synthetic (red) traces for 18 events from shotline 26; the traces only include the first 700 ms of data after the onset of the first arrival (black line on each trace).

VI. Conclusions and future directions

- **This study represents the first application of acoustic anisotropic 3D FWI to an academic OBS dataset. We show that FWI is capable of recovering velocity anomalies with a resolution 2-4 times better than conventional travel time tomography when using a non-optimal, academic-sized data set.**
- Velocity variations beneath the five large hydrothermal vent fields are consistent with ongoing fracturing and mineral precipitation within the hydrothermal reaction zone.
- The low-velocity anomaly on the northern end of the Endeavour segment indicates a region of enhanced porosity and permeability caused by recent earthquake swarms in the region[2].
- Results are promising. Current inversions incorporate a subset of the data within 2.9 to 15 km offset from the receiver to avoid noise present in the lower frequencies at larger offsets (Fig. 4). At higher frequencies (>4.5 Hz), however, data at larger offsets contain less noise and can be used in future inversions to improve model resolution.
- Continued assessment of the pre-processing of the field data is required to improve the model resolution and overall fit between the field data and synthetics. For instance, using larger mute windows (e.g. 1000 vs. 700 ms) will provide greater depth resolution and adjusting the onset time of the top mute will improve the match of the resulting synthetics to the field data; this may be applicable to the large phase residuals within the 2.9-15 km offset range (Fig. 7a), which may be caused by noise preceding the onset time of the first arrivals. Additional evaluation of the field quality input into FWI is also required to remove any noisy or cycle-skipped traces.